Snow Grain Size Retrieval over the Polar Ice Sheets with the Ice, Cloud, and land Elevation Satellite (ICESat) Observations

Yuekui Yang[1, 2], Alexander Marshak[2], Mei Han[2,3],
Stephen P. Palm[2,4], David J. Harding[2]

Submitted to

Journal of Quantitative Spectroscopy and Radiative Transfer

[1]Universities Space Research Association, Columbia, MD.

[2]NASA Goddard Space Flight Center, Greenbelt, MD.

[3]Morgan State University, Baltimore, Maryland

[4]Science Systems and Applications Inc., Lanham, MD

Abstract

Snow grain size is an important parameter for cryosphere studies. As a proof of concept, this paper presents an approach to retrieve this parameter over Greenland, East and West Antarctica ice sheets from surface reflectances observed with the Geoscience Laser Altimeter System (GLAS) onboard the Ice, Cloud, and land Elevation Satellite (ICESat) at 1064 nm. Spaceborne lidar observations overcome many of the disadvantages in passive remote sensing, including difficulties in cloud screening and low sun angle limitations; hence tend to provide more accurate and stable retrievals. Results from the GLAS L2A campaign, which began on 25 September and lasted until 19 November, 2003, show that the mode of the grain size distribution over Greenland is the largest (~300 μm) among the three, West Antarctica is the second (~220 μm) and East Antarctica is the smallest (~190 μm). Snow grain sizes are larger over the coastal regions compared to inland the ice sheets. These results are consistent with previous studies. Applying the broadband snow surface albedo parameterization scheme developed by Garder and Sharp (2010) to the retrieved snow grain size, ice sheet surface albedo is also derived. In the future, more accurate retrievals can be achieved with multiple wavelengths lidar observations.

1. Introduction

As a fundamental parameter of the snowpack, grain size has long been recognized as an important factor in understanding and predicting the status of the ice sheets (e.g., Refs. [1-3]). Satellite remote sensing has enabled quantitative grain size mapping from space and significant progress has been made in the field (e.g., Refs. [4-6]). The theoretical basis is that in the near infrared (NIR) and shortwave infrared (SWIR) region absorption is a function of snow grain size. Larger grains result in larger absorption hence smaller reflectance [7]. To the best of our knowledge, the snow grain size retrieval methods presented in the past literature were all based on passive remote sensing observations. These methods rely on surface reflected sunlight for the retrievals and large uncertainties can arise from the low sun angle over the polar regions. This is because not only a low sun causes more difficulties to the already challenging task of atmospheric correction, it also intensifies the effect of surface roughness because of the shadows. In addition, the small contrast between surface and clouds in both the thermal and visible spectra makes clouds screening very difficult for passive remote sensing and hence results in uncertainties as well (e.g., Refs. [8-10]).

Active remote sensing observations from the Geoscience Laser Altimeter System (GLAS) onboard the Ice, Cloud,and land Elevation Satellite (ICESat) provide an opportunity to retrieve snow grain size that is much less affected by the above mentioned uncertainty factors. The GLAS lidar used the 1064 nm wavelength for its surface elevation measurements. At this wavelength, snow absorption is large enough so that the grain size signal is detectable from the lidar ground returns. Figure 1 gives the imaginary part of the refractive index for ice particles as a function of wavelength [22], which can be regarded as a measure of absorption strength. Compared to a 532nm laser, the imaginary part of the ice refractive index at 1064 nm is 3 orders of magnitude larger.

Over the polar regions, retrieving grain size using space-borne lidar observations has many advantages: (1) unlike passive remote sensing, cloud screening over ice sheets is essentially not a problem for lidar observations; (2) for lidar observations, the overhead light source minimizes the surface roughness effect and hence lower the uncertainties in the retrieval; (3) not restrained by the availability of sunlight, retrievals with lidar data can be done both day and night; (4) atmospheric correction is critical to the retrieval process and it is a difficult task for passive remote sensing because of the low sun angle; for active remote sensing, the nadir observing geometry minimizes the path length through the atmosphere and makes atmospheric correction more accurate.

Snow grain size retrievals are based on surface reflectivity. We note that even though widely applied to climate and earth system research, data from the Cloud-Aerosol Lidar and Infrared Pathfinder Satellite Observation (CALIPSO) are not suitable for snow grain size retrieval, because the surface return saturates the detectors under clear sky conditions over the polar ice sheets.

The remainder of the paper is organized as follows: Section 2 introduces the data and the methodology used for this study; Section 3 describes the snow grain size retrieval results; in Section 4, ice sheet surface albedo is derived from the snow grain size retrievals; and the results are summarized in Section 5.

2. Data and Methodology

2.1 Surface bidirectional reflectance factor (BRF) from the GLAS 1064 nm lidar

The GLAS lidar was launched on board ICESat in January 2003. It has three lasers. To extend the lifetime of the mission, GLAS operated in a campaign mode with each campaign lasting about one to two months. It has two channels, one at 1064 nm and one at 532 nm. The 532 nm channel is designed for atmospheric observations, while the 1064 nm one is for surface elevation measurements [11] [12]. The laser transmits pulses at 40 Hz which gives a nominal 172 m footprint spacing along track. With GLAS, a bidirectional reflectance factor (BRF) value can be derived from the energy received within the surface range gate. This value is called the apparent surface reflectance (ASR) because it is the product of the two-way transmittance of the atmosphere and the true surface BRF [13]. ASR is calculated as:

$$\rho_{app}(\mu_0,\mu,\varphi) = \frac{\pi L(\mu_0,\mu,\varphi)}{\mu_0 F_{emit}} \qquad (1)$$

where L is the radiance at the sensor resulted from the photons reflected by the surface; μ_0 and μ are the cosine of illumination zenith angle and view zenith angle, respectively (for GLAS, $\mu_0 = \mu = 1.0$); φ is the relative azimuth angle; F_{emit} is the emitted laser energy flux in W/m^2.

ASR is archived as a GLAS product. For this study, we use the data from the GLAS campaign L2A, which is the first GLAS campaign with full on-orbit operation of the instrument. The L2A campaign began on 25 September and lasted until 19 November 2003. Some of L2A returns were saturated, especially during the early part of the campaign when the laser energy was higher. The ASR product has a received energy correction applied bases on laboratory calibration data. Figure 2 shows the distributions of all sky ASR during this campaign period over the polar ice sheets, including Greenland, East and West Antarctica. In the figure, the peaks on the right represents clear sky observations. We selected the L2A campaign because during this period GLAS had a fully functional atmosphere channel and the best cloud detection capability [11]; hence cloud screening is the most accurate among all the GLAS campaigns.

To retrieve grain size, snow surface BRF needs to be obtained. It is a straightforward process for GLAS. First we separate the scenes into cloudy and clear based on the ICESat cloud detection results [11][14]. Then, atmospheric correction is done by dividing the clear sky ASR by the Rayleigh two-way transmittance. Only clear sky observations are used for the retrievals.

2.2 The Analytical Asymptotic Radiative Transfer (AART) model

The general approach of snow grain size retrieval is to employ a radiative transfer model and build a look up table, in which the surface reflectivity at the NIR/SWIR region is calculated as a function of grain size, light incidence angle and view angle. In this study, we adopt the Analytical Asymptotic Radiative Transfer (AART) model developed by Kokhanovsky and Zege [15]. This model accounts for irregular shapes of the snow grains and has been validated with ground observations [21]. It has been applied to retrievals with the MODerate-resolution Imaging Spectroradiometer (MODIS) data [4] [5]. The model is also applicable to lidar observations [13].

We define the snow grain size as the effective diameter of the grains, which is the ratio of the average volume to the average surface area. Snow grains are assumed fractals. Based on the AART model, the surface BRF ρ can be related to the snow grain size d through:

$$\rho(\mu_0,\mu,\varphi) = R_0(\mu_0,\mu,\varphi)\exp(-A(\mu_0,\mu,\varphi)\sqrt{\gamma d}) \qquad (2)$$

where

$$A(\mu_0,\mu,\varphi) \cong 0.66(1+2\mu_0)(1+2\mu)/R_0(\mu_0,\mu,\varphi) \quad (3)$$

and

$$\gamma = 4\pi\chi/\lambda \quad (4)$$

where μ_0, μ and φ are the same as in Equation (1); λ is the wavelength; d is the effective diameter of the snow particles; χ is imaginary part of the refractive index and R_0 is the BRF for semi-infinite media with no absorption. Here R_0 is calculated with the snow reflectance model developed by Mishchenko et al. [17].

Figure 3 shows the snow BRF for different grain sizes as a function of wavelength calculated with the AART model with overhead light source and nadir view. As can be seen from the figure, the clear separation of BRF for different grain sizes at 1064 nm provides the foundation for the retrievals.

3. Snow Grain Size over the Polar Ice Sheets

Equation 2 relates the GLAS surface BRF measurements at 1064 nm to snow grain size. Based on this, retrievals are done for the data from the GLAS L2A campaign. Ideally, the reflectance model should consider the absorbing aerosol deposition, but over the polar ice sheets, its effect is very small [4]; hence it is not considered it in this study.

Results of snow grain size retrievals for the L2A campaign over Greenland and Antarctica are displayed in Figure 4. As shown in the figure, snow gains are generally larger towards the edge of the ice sheets. Grain sizes are also larger over Greenland than over Antarctica. Figure 5 shows the grain size distribution histograms. The mode of the distribution over Greenland is the largest (~300 μm) among the three, West Antarctica is the second (~220 μm) and East Antarctica is the smallest (~190 μm). Snow on the ground experiences metamorphism and the grain size and shape changes as a function of temperature, pressure and age. The general pattern and the value range of the results shown here are consistent with previous studies [4][16][18].

4. Snow Surface Albedo

Snow surface albedo is a critical player in the ice sheet surface energy budget, and subsequently in snowmelt and in surface mass balance. To derive snow surface albedo from grain size, we adopt the parameterization scheme developed by Garder and Sharp [19], where the clear-sky broadband snow surface albedo α is calculated as a function of snow grain size, solar zenith angle, and snow impurities:

$$\alpha = \alpha_s + \alpha_\mu + \alpha_c \qquad (5)$$

where α_s is the base albedo due to snow grain size, α_μ and α_c represent the effects of solar zenith angle and snow impurities.

$$\alpha_s = 1.48 - 1.21031 d^{0.07} \qquad (6)$$

where d is the snow grain size.

$$\alpha_\mu = 0.53\alpha_s(1-\alpha_s)(1-\mu_s)^{1.2} \qquad (7)$$

where μ_s is the cosine of the solar zenith angle.

Since the effect of impurities is very small over the polar ice sheet [4], it is not considered here; hence:

$$\alpha_c = 0 \qquad (8)$$

This parameterization has been implemented and tested by Kuipers Munneke et al. [20] and good agreement has been achieved between the modeled and observed albedo.

With Equations 5 to 8, clear sky albedo can be directly calculated for different solar zenith angles from the grain size retrievals shown in Figure 4. Figure 6 shows the clear-sky albedo for a 60° solar zenith angle. As can be seen from the figure, for the same solar zenith angle, Antarctica appears brighter (larger albedo) than Greenland and the inner parts of the ice sheets are also generally brighter than the coastal areas. The reason is that larger grain sizes lead to smaller surface albedo (Equation 6). Figure 7 shows the histograms of the clear-sky albedo given in Figure 6. For the case shown here, the modes of clear sky albedo are 0.83, 0.84, and 0.85 for Greenland, East and West Antarctica, respectively.

5. Summary and Discussions

Observations of the GLAS 1064 nm lidar provide an opportunity to retrieve snow grain size with advantages that are not available to passive remote sensing techniques. First, lidar observations are sensitive to clouds; hence cloud screening is much more accurate than for passive remote sensing over bright surfaces; second, the overhead light source minimized the impact of surface roughness on the retrievals; third, lidar observations minimizes the photon path length through the amtopshere resulting atmosphere correction more accurate; also, retrievals with lidar data can be done for both day and night, while current passive remote sensing techniques require sunlight.

This paper adopts the AART model developed by Kokhanovsky and Zege [15] and snow grain size over the polar ice sheets are retrieved for the period of the GLAS L2A campaign (from 25 September to 19 November, 2003). Results show that the mode of the grain size distribution over Greenland is ~300 µm; it is ~220 µm over West Antarctica and ~190 µm over East Antarctica. Snow grain sizes are larger over the coastal regions compared to inland the ice sheets. Applying the broadband snow surface albedo parameterization scheme developed by Garder and Sharp [19] to the retrieved snow grain size, ice sheet surface albedo is also derived using a 60° solar zenith angle as an example. Results show that the modes of clear sky albedo are 0.83, 0.84, and 0.85 for Greenland, West and East Antarctica, respectively. These results can be used as input for numerical models and are helpful in understanding the surface energy budget over the polar regions.

We note that this study is a proof of concept. The AART model, even though extensively validated under different conditions, has not been directly validated at the direct backscattering direction, known as hot spot, due to lack of observations at this particular geometry. Potential model uncertainties at the hot spot direction may result in errors in the retrievals. In addition, retrievals from single channel observations require high accuracy in absolute calibration. To achieve better retrievals, multi wavelength lidar observations, such as the ones made the Slope Imaging Multi-polarization Photon-counting Lidar (SIMPL) [23, 24], are needed. SIMPL acquired data over a range of grain size conditions in Greenland during July and August 2015. Once calibrated, this method can be applied and compared to grain size retrievals being made from the co-flying hyperspectral instrument Next-Generation Airborne Visible/Infrared Imaging Spectrometer (AVIRISng) [25].

Acknowledgements:

This study is supported by the NASA ICESat-2 Science Definition Program under the grant NNX15AE87G. The authors thank Drs. Alexander Kokhanovsky for helpful discussions. We also appreciate the helpful comments and suggestions from two anonymous reviewers.

References

[1] Massom, R. A., and D. Lubin, 2006: Polar remote sensing volume II: Ice sheets. Chichester/Berlin: Praxis/Springer, 426 pp.

[2] Nolin, A. W., and J. Stroeve, 1997: The changing albedo of the Greenland ice sheet: Implications for climate modeling. *Ann. Glaciol.*, **25,** 51–57.

[3] Warren, S. G., 1982: Optical properties of snow, *Rev. Geophys.*, 20, 67–89.

[4] Lyapustin, A., M. Tedesco, Y. Wang, T. Aoki, M. Hori, and A. Kokhanovsky, 2009: Retrieval of snow grain size over Greenland from MODIS, *Remote Sens. Environ.*, 113, 1976–1987, doi:10.1016/j.rse.2009.05.008.

[5] Scambos, T. A., T. M. Haran, M. A. Fahnestock, T. H. Painter, and J. Bohlander, 2007: MODIS-based Mosaic of Antarctica (MOA) data sets: Continent-wide surface morphology and snow grain size, *Remote Sens. Environ.*, 111(2–3), 242–257.

[6] Nolin, A., and J. Dozier, 2000: A hyperspectral method for remotely sensing the grain size of snow, *Remote Sens. Environ.,* 74(2), 207–216

[7] Wiscombe, W. J., and S. G. Warren, 1980: A model for the spectral albedo of snow. I: Pure snow. *J. Atmos. Sci.,***37,** 2712–2733.

[8] Yang, Y. and L. Di Girolamo, 2008: Impacts of 3-D Radiative Effects on Satellite Cloud Detection and Their Consequences on Cloud Fraction and Aerosol Optical Depth Retrievals. *J. Geophys. Res.,* 113, D04213, doi:10.1029/2007JD009095.

[9] Yang, Y., L. Di Girolamo and D. Mazzoni, 2007: Selection of the automated thresholding algorithm for Multi-angle Imaging SpectroRadiometer Radiometric Camera-by-Camera Cloud Mask over land. *Remote Sens. Environ.*. 107, 159-171, doi:10.1016/j.rse.2006.05.020.

[10] Ackerman, S. A., K.I. Strabala, W.P. Menzel, R.A. Frey, C.C. Moeller and L.E. Gumley, 1998: Discriminating clear sky from clouds with MODIS. *J. Geophys. Res.,* 103(D24): 32141-32157.

[11] Spinhirne, J.D., S.P. Palm, W.D. Hart, D.L. Hlavka, and E.J. Welton, 2005: Cloud and aerosol measurements from GLAS: Overview and initial results. *Geophys. Res. Letters*, **32** (22), L22S03, doi:10.1029/2005GL023507.

[12] Yang, Y., A. Marshak, J. C. Chiu, W. J. Wiscombe, S. P. Palm, A. B. Davis, D. A. Spangenberg, L. Nguyen, J. D. Spinhirne, and P. Minnis, 2008: Retrievals of Thick Cloud Optical Depth from the Geoscience Laser Altimeter System (GLAS) by Calibration of Solar Background Signal. *Journal of Atmospheric Sciences*. 65, 3513–3527.

[13] Yang, Y., A. Marshak, S. Palm, Z. Wang, C. Schaaf, 2013: Assessment of Cloud Screening with Apparent Surface Reflectance in Support of the ICESat-2 Mission. *IEEE Trans. Geos. Remote Sens*., 51(2), 1037-1045, doi: 10.1109/TGRS.2012.2204066.

[14] Palm, S. P., J. D. Spinhirne, W. D. Hart, and D. L. Hlavka, 2002: GLAS atmospheric data products, algorithm theoretical basis document, version 4.2, GSFC, Greenbelt, Md. (Available at: http://www.csr.utexas.edu/glas/pdf/glasatmos.atbdv4.2.pdf.).

[15] Kokhanovsky, A. and E. P. Zege, 2004: Scattering optics of snow. *Appl. Opt.*, 43, 1589−1602.

[16] Tedesco, M., A. Kokhanovsky, 2007: The semi-analytical snow retrieval algorithm and its application to MODIS data, *Remote Sens. Environ*., 111, 228–241.

[17] Mishchenko, M.I., J.M. Dlugach, E.G. Yanovitskij, and N.T. Zakharova, 1999: Bidirectional reflectance of flat, optically thick particulate layers: An efficient radiative transfer solution and applications to snow and soil surfaces. *J. Quant. Spectrosc. Radiat. Transfer*, **63**, 409-432, doi:10.1016/S0022-4073(99)00028-X.

[18] Gay, M., M. Fily, C. Genthon, M. Frezzotti, H. Oerter, and J-G. Winther, 2002: Snow grain-size measurements in Antarctica. *J. Glaciol.*, **48,** 163, 527–535.

[19] Gardner, A. S., and M. J. Sharp, 2010: A review of snow and ice albedo and the development of a new physically based broadband albedo parameterization, *J. Geophys. Res.*, 115, F01009, doi:10.1029/2009JF001444.

[20] Kuipers Munneke, P., M. R. van den Broeke, J. T. M. Lenaerts, M. G. Flanner, A. S. Gardner, and W. J. van de Berg, 2011: A new albedo parameterization for use in climate models over the Antarctic ice sheet, *J. Geophys. Res.*, 116, D05114, doi:10.1029/2010JD015113.

[21] Kokhanovsky, A. A. and M. Schreier, 2009: The determination of snow specific area, albedo and effective grain size using AATSR spaceborne observations, Int. J. Remote Sens., 30(4), 919–933.

[22] Warren, S.G., 1984. Optical constants of ice from the ultraviolet to the microwave. *Applied optics*, *23*(8), pp.1206-1225.

[23] Dabney, P., D. Harding, J. Abshire, T. Huss, G. Jodor, R. Machan, J. Marzouk, K. Rush, A. Seas, C. Shuman, X. Sun, S. Valett, A. Vasilyev, A. Yu and Y. Zheng, 2010: The Slope Imaging Multi-polarization Photon-counting Lidar: Development and

performance results, *2010 IEEE International Geoscience and Remote Sensing Symposium (IGARSS),* 653-656, [10.1109/IGARSS.2010.5650862].

[24] Harding, D., P. Dabney, S. Valett, A. Yu, A. Vasilyev and A. Kelly, 2011: Airborne polarimetric, two-color laser altimeter measurements of lake ice cover: A pathfinder for NASA's ICESat-2 spaceflight mission, *2010 IEEE International Geoscience and Remote Sensing Symposium (IGARSS)*, 3598-3601, [10.1109/IGARSS.2011.6050002].

[25] Brunt, K.M., Neumann, T.A. and Markus, T., 2015: SIMPL/AVIRIS-NG Greenland 2015 Flight Report, NASA/TM–2015-217544.

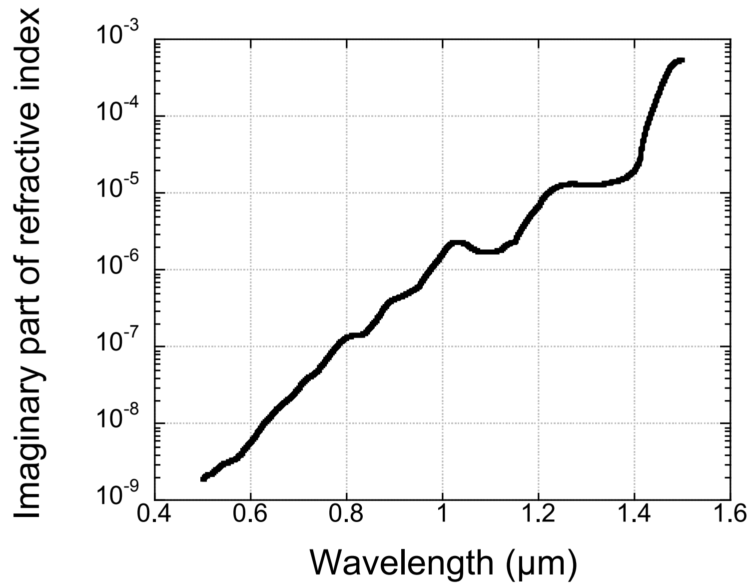

Figure 1. The imaginary part of refractive index for ice as a function of wavelength.

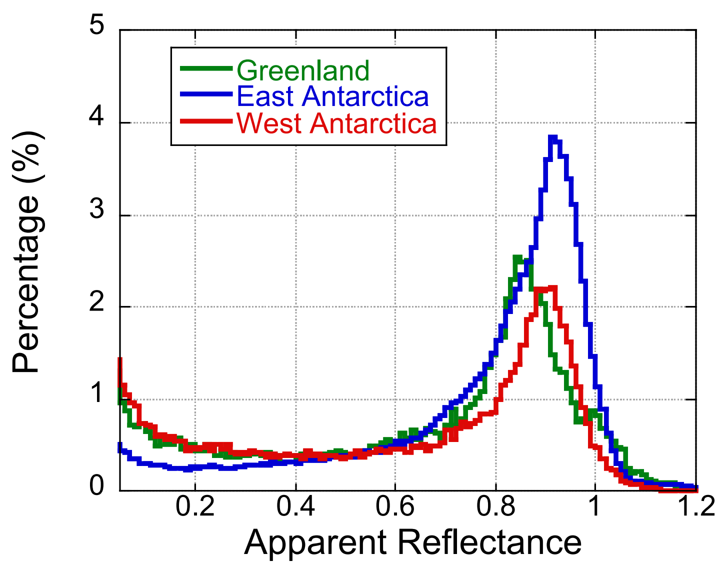

Figure 2. Distributions of all sky apparent reflectance observed during the GLAS L2A campaign conducted from 25 September to 19 November, 2003. Lines are for Greenland (green), East Antarctica (blue) and West Antarctica (red).

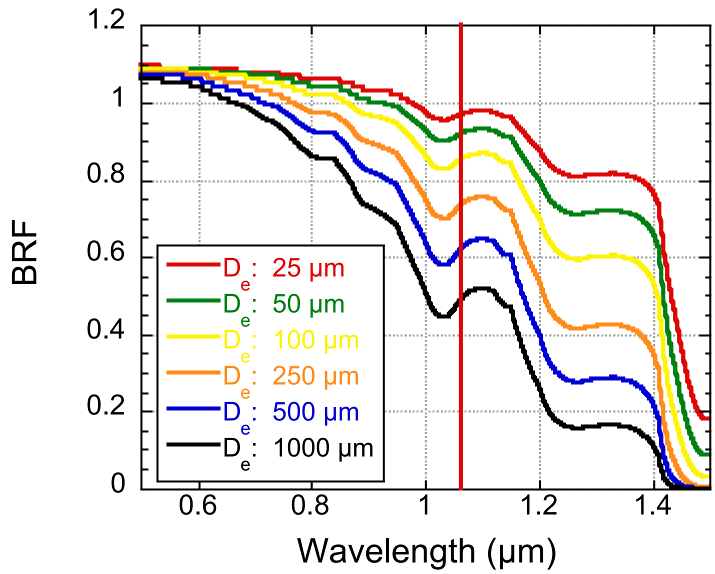

Figure 3. Snow BRF for different grain sizes as a function of wavelength calculated with the AART model with overhead light source illumination and nadir view. The vertical red line marks the position of the 1064 nm wavelength.

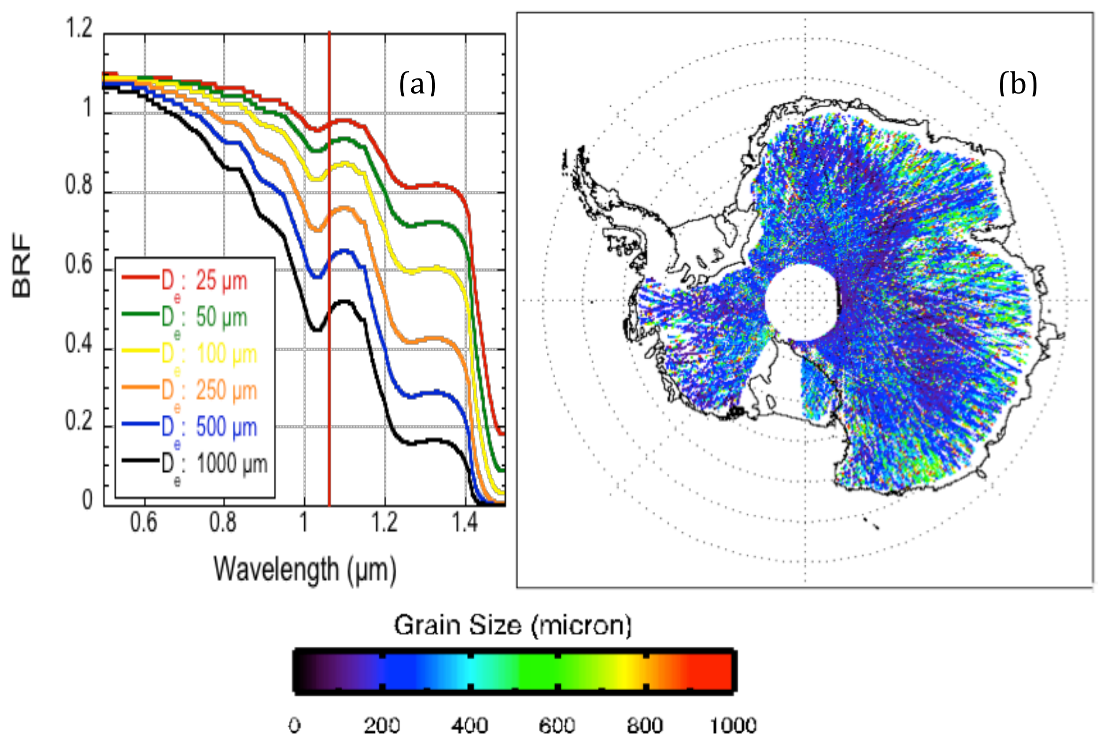

Figure 4. Snow grain sizes retrieved with observations from the GLAS L2A campaign. (a) Retrievals over the Greenland ice sheet; (b) retrievals over the Antarctica ice sheet.

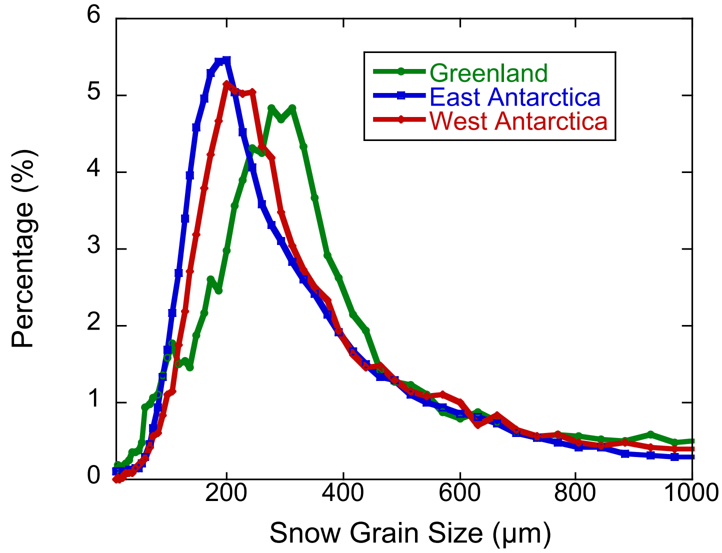

Figure 5. Histograms of snow grain size distribution over the ice sheets retrieved with GLAS observations during the GLAS L2A campaign. Lines are for Greenland (green), East Antarctica (blue) and West Antarctica (red).

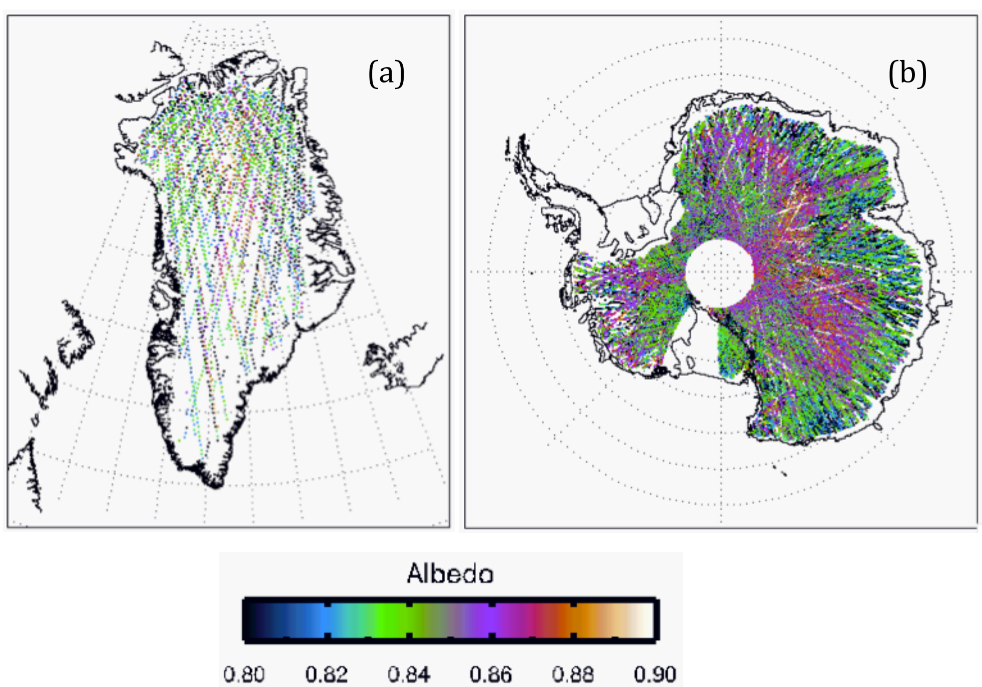

Figure 6. Surface albedo derived from the snow grain size retrieved with data from the GLAS L2A campaign. Solar zenith angle is assumed 60º. (a) The Greenland ice sheet; and (b) the Antarctica ice sheet.

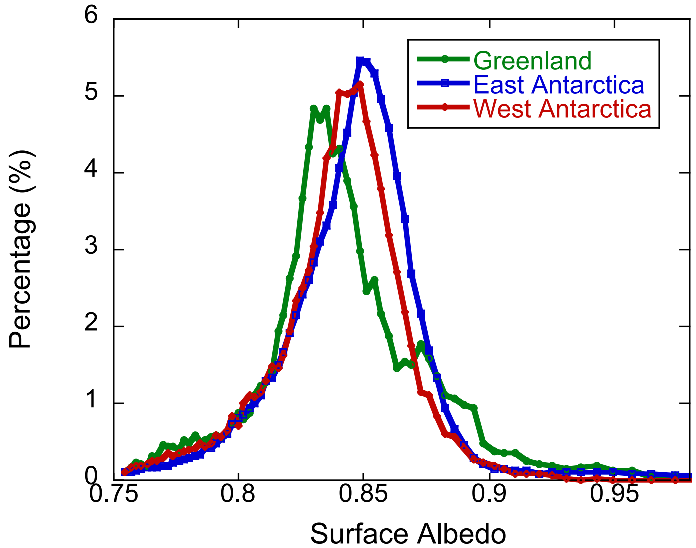

Figure 7. Histograms of surface albedo derived from the snow grain size retrieved with data from the GLAS L2A campaign. Solar zenith angle is assumed 60º.. Lines are for Greenland (green), East Antarctica (blue) and West Antarctica (red).